JACS
JOURNAL OF THE AMERICAN CHEMICAL SOCIETY

Article

Catalyst-Controlled Diastereoselective Synthesis of Cyclic Amines via C-H Functionalization

Sailu Munnuri, Adeniyi Michael Adebesin, Mahesh P Paudyal, Muhammed Yousufuddin, Alfonso Dalipe, and John R. Falck

J. Am. Chem. Soc., **Just Accepted Manuscript** • DOI: 10.1021/jacs.7b09901 • Publication Date (Web): 28 Nov 2017

Just Accepted

ACS Publications

Journal of the American Chemical Society is published by the American Chemical Society. 1155 Sixteenth Street N.W., Washington, DC 20036

Catalyst-Controlled Diastereoselective Synthesis of Cyclic Amines via C-H Functionalization

Sailu Munnuri,[1] Adeniyi Michael Adebesin,[1] Mahesh P. Paudyal,[1] Muhammed Yousufuddin,[2] Alfonso Dalipe[2] and John R. Falck[1,*]

[1]Division of Chemistry, Departments of Biochemistry and Pharmacology, University of Texas Southwestern Medical Center, Dallas, TX 75390, USA; [2]Life and Health Sciences Department, University of North Texas at Dallas, Dallas, TX 75241, USA

ABSTRACT: Reliable regio- and stereochemical techniques applicable to non-activated aliphatic systems remain largely elusive due to the challenges of discriminating between multiple, relatively strong sp^3 C-H bonds whose chemical behavior often differ only subtly. Nevertheless, approaches that employ directing groups and/or auxiliaries have emerged, but impose practical restrictions, especially in complex molecule synthesis. This report describes a catalyst-controlled regio- and diastereoselective synthesis of *N*-unprotected pyrrolidines via dirhodium catalyzed intramolecular nitrene insertion into sp^3 C-H bonds. The reaction proceeds at rt without external oxidants, nitrene stabilizing groups, or directing functionality. The insights that emerged from the conformational/stereoselectivity relationships (CSR) between catalysts and substrates provide a framework for rational catalyst design that can accommodate a broader range of aliphatic C-H chemistry.

INTRODUCTION

Few bond forming reactions possess the minimalist appeal of direct C-H activation with its implied economies, range, and site-/stereo-selectivities, even if these are not yet fully realized. An application of high priority is the preparation of cyclic amines which recognizes the prominence of this functionality in pharmaceuticals and other commercially important substances[1,2] (Figure 1) and the limitations of traditional synthetic cycloamine methodology, *inter alia*, nucleophilic substitution, rearrangements, cycloadditions, and reductive amination.

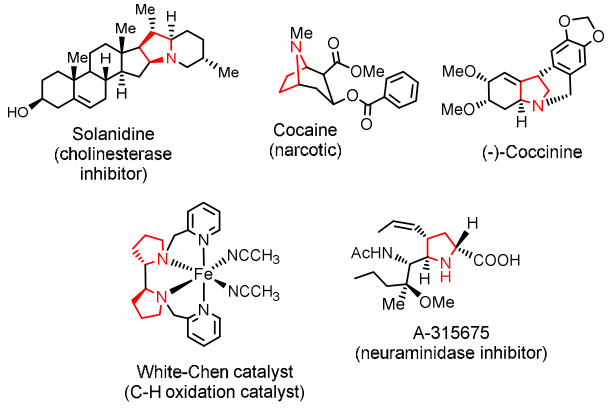

Figure 1. Pyrrolidine containing natural products and commercially important compounds.

Recent advances in the direct activation of sp^2 and sp^3 hydrogens have enabled access to cyclic amines of various ring sizes from readily available and simple starting materials.[3-8] However, transition metal-mediated sp^3 C-H activation, which enables the functionalization of saturated hydrocarbons, is typically more challenging than sp^2 C-H activation.[9] Synthetic utility is further restrained by the chemical equivalency of many sp^3 C-H bonds, particularly in non-branched aliphatic chains.

Innovative work by Gaunt,[10] Shi,[11] Chen,[12] and Daugulis[13] provide access to aziridines, azetidines, and pyrrolidines via amination of sp^3 C-H bonds. Most of the above procedures including the Suárez modification to the Hofmann-Löffler-Freytag (HLF) reaction[14-16] require an external oxidant, but unlike the HLF reaction, utilize transition metals and, in most cases, *N*-protecting groups and elevated reaction temperatures. The state of the art for cyclic amine synthesis via sp^3 C-H insertion was recently redefined by reports from the Betley[17] and the van der Vlugt[18,19] laboratories using redox active catalysts. Both, however, (i) required *in situ* ^{t}Boc derivatization of the amine product when conducted in the catalytic mode, (ii) were conducted at elevated temperatures and (iii) provided diastereoselectivities ranging from 1:1 to 3.9:1. Herein, we report the highly diastereoselective, direct insertion of a non-stabilized nitrenoid into sp^3 C-H bonds at rt to furnish either *N*-unprotected *cis*- or *trans*-2,5-disubstituted pyrrolidines based upon the identity of the catalyst (Scheme 1).

Scheme 1. Insertion of Nitrogen into sp³ C-H Bonds.

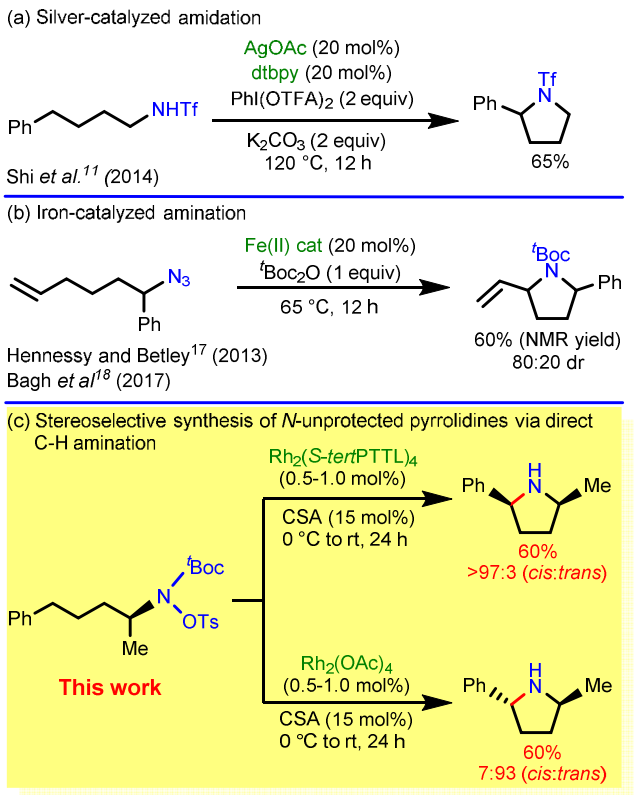

RESULTS AND DISCUSSION

Our prior explorations into the eccentricities of *N*-unprotected Rh-nitrenoids and their applications to aziridination[7] and aryl amination[20] led us to examine their potential for intramolecular insertion into unactivated sp³ C-H bonds (Scheme 2). Under the standard conditions established for our direct arene amination methodology, **1a** was completely consumed within 2 hours at 0 °C, and the intramolecular insertion product **2a** was obtained in moderate yield (40%) after isolation as its *N*-tosylamide. The preference for the kinetic five-membered pyrrolidine was determined spectroscopically and confirmed by later studies.

Scheme 2. Initial Investigation of Direct Intramolecular Rh_2-nitrenoid Insertion into an Unactivated sp³ C-H Bond.

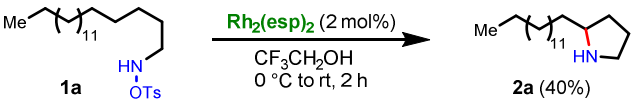

A notably improved yield of pyrrolidine (from 40% to 60%) was realized via *in situ* deprotection[20] of the ᵗBoc-protected analog of **1a** (Scheme 3, **1b**→**2b**), although a longer reaction time was required for complete conversion to product. The increased yield is attributed to the gradual generation of the nitrenoid precursor as the ᵗBoc is cleaved, which minimizes shunting to unproductive, non-metal mediated side reactions such as aldehyde formation. In the absence of acid, the ᵗBoc remained and insertion was not observed; starting material **1b** was recovered after 24 h. Further examination of the substrate scope (Scheme 3) using this modification continued with the conformationally locked equatorial **1c** and axial **1d** which smoothly inserted to furnish **2c** and **2d**, respectively, with ≥99% stereospecificity as judged by NMR analysis of the crude reaction mixtures, a process most consistent with a concerted insertion into the spiro-methine C-H. A brief examination of reaction preference revealed insertion into a benzylic C-H (**1e**→**2e**) took precedence over aryl amination and formation of pyrrolidines **2f** and **2g** were favored over piperidine options, although the latter methine example was somewhat sluggish. If insertion into a δ-C-H is blocked, then ε-methylene insertion is a viable alternative (**1h**→**2h**). These results emphasize the importance of kinetic control in predicting the product distribution of this Rh-nitrenoid addition into sp³ C-H bonds. Additionally, the preference for methylene versus methyl insertion as seen in **2h** also signifies a partial thermodynamic contribution (differences in bond strengths) to product selectivity.

Many functional groups were compatible, e.g., ketones (**2i**) hydroxyl (**2j**), arylamides (**2k**,**l**) and ester (**2m**), although the latter was accompanied by some transesterification (10-15%) with the trifluoroethanol solvent. Notably, we did not notice aromatization during the transformation of the redox sensitive indoline **1k**. Alkyl amides, however, interfere with pyrrolidine formation and α-insertion leading to carbonyls predominates (SI). Significantly, more complex structures were also accessible including the nortropane alkaloid **2n**, adamantanopyrrolidine **2o** (previously prepared in 6 steps[21]) and the late stage example, **2p**, a representative of the solanidine class of steroidal alkaloids (Figure 1). The structure of **2p** was confirmed by X-ray crystallography. It is of interest that for the transannular closure to **2n** a survey of commercial and non-commercial catalysts revealed that the homoleptic dirhodium catalyst derived from dehydroabietic acid (DBA) provided superior yields of **2n** and reduced cycloheptanone formation compared to other tetracarboxylate catalysts including $Rh_2(esp)_2$. This result is especially impressive given the difficulties associated with transannular C-H aminations to form medium sized rings.[22,23] The observed reduction in α-insertion could be due to favorable interactions between the DBA ligands around the dirhodium catalyst and the substrate which increase the population of (or stabilize) the boat conformer required for productive conversion to product.

Despite the impressive progress in extending the utility of nitrene insertions with the introduction of stabilizing functionality and directing/coordinating groups,[24-27] there are no highly diastereoselective, direct sp³ C-H insertions leading to *N*-unprotected small rings. High selectivities are particular important when considering the cost and difficulties associated with chromatographic separation of product mixtures on a preparative scale. Attention was, therefore, directed at the initial development of a preferential preparation of either *cis*- or *trans*-pyrrolidines controlled by catalyst selection for maximum operational flexibility. To this end, a range of commercial and non-

Scheme 3. Intramolecular Amination of sp³ C-H Bonds.

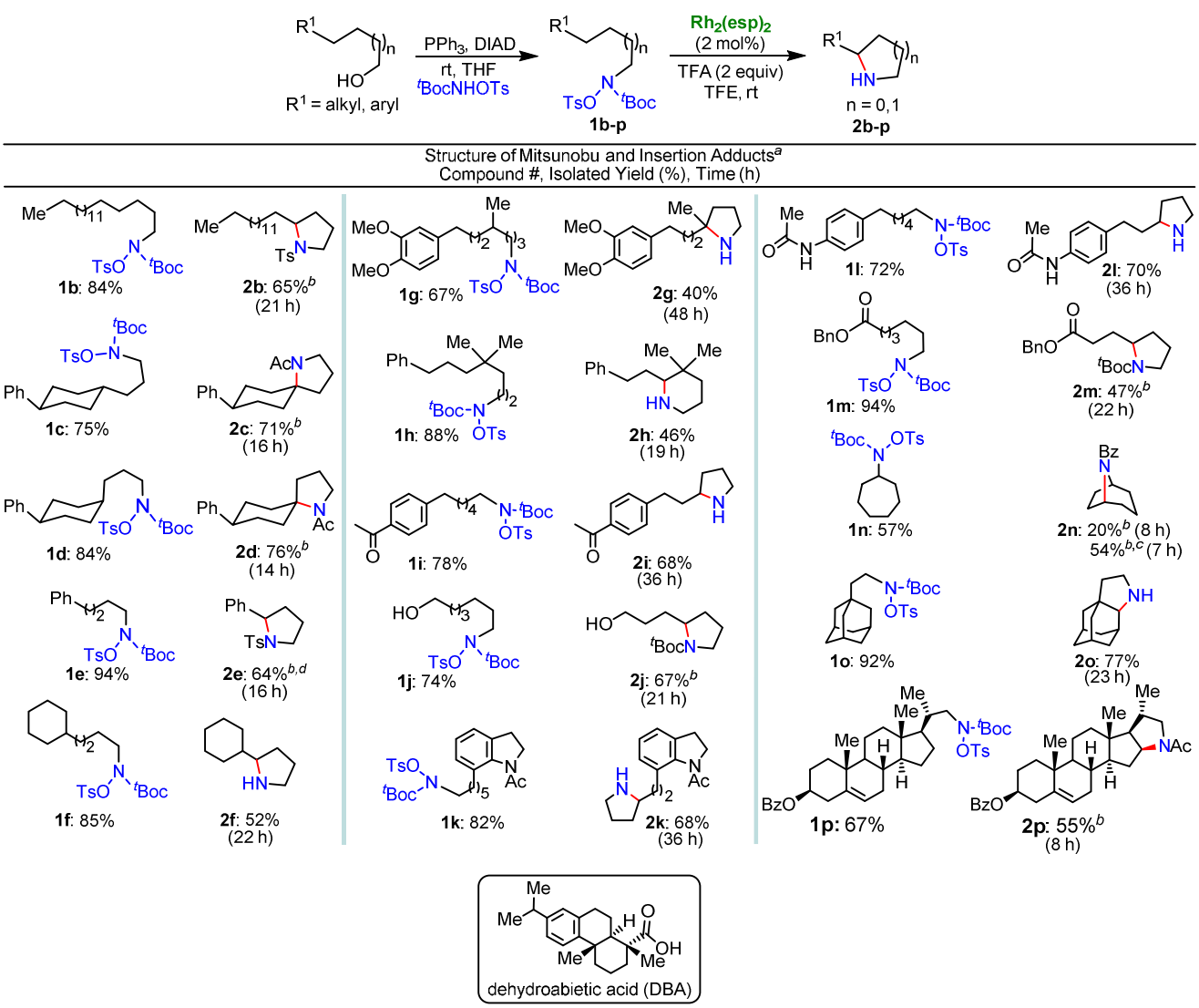

[a]Reaction conditions: $Rh_2(esp)_2$ (2 mol%), F_3CCO_2H (2 equiv), F_3CCH_2OH (TFE) as solvent, rt. [b]Derivatized for ease of isolation. Combined yield for 2 steps. [c]$Rh_2(DBA)_4$ (1 mol%) instead of $Rh_2(esp)_2$. DBA = dehydroabietic acid.[d] α,α,α-Trifluorotoluene (TFT)/TFE (1:1).

commercial dirhodium catalysts was evaluated using **3a** as the model substrate (Table 1). It became clear that carboxylate ligands were superior in yield to carboxamidate ligands (see SI). Also, despite the expectation that the diastereotopic transition states arising from matched and mismatched interactions between the chiral substrate **3a** and chiral dirhodium catalysts would influence the stereochemical results, no significant effect was observed (see SI Tables 2 and 3), except a modest difference (1:1 vs. 1:4) with the highly congested cyclopropanecarboxylate catalyst[28] $Rh_2(BTPCP)_4$. Furthermore, reaction optimization studies showed that catalytic amounts of camphorsulfonic acid (CSA, 15 mol%) instead of trifluoroacetic acid and the use of α,α,α-trifluorotoluene (TFT) or CH_2Cl_2 as co-solvents with trifluoroethanol gave more reproducible diastereoselectivities and reaction times. Therefore, these conditions were adopted in subsequent experiments. As the representative examples in Table 1 reveal, most dirhodium carboxylate catalysts favor *trans*-**4a**, with an inverse relationship between *trans*-selectivity and steric bulk of the ligands around the dirhodium catalyst. The readily available $Rh_2(S\text{-DOSP})_4$ and $Rh_2(OAc)_4$ catalysts (entries 4 and 8) showed the best *trans*-selectivities, albeit the later proved to be the more selective catalyst as well as the most cost effective. On the other hand, catalysts which adopt the chiral crown conformation[29-31] favored *cis*-**4a** (entries 6 and 7). Catalyst $Rh_2(S\text{-}tert\text{PTTL})_4$, introduced by Ghanem and co-workers, afforded the highest *cis*-selectivity and generated *cis*-**4a** with superb specificity versus *trans*-**4a**. A compelling rationale for the differences in diastereoselectivity between $Rh_2(S\text{-}tert\text{PTTL})_4$ and $Rh_2(PTAD)_4$, despite their similar conformations and structures, could evolve from their different cavity sizes.[31] This hypothesis has not been well appreciated in the design of dirhodium catalysts for nitrene insertions and provides a promising avenue for the further development

Table 1. Influence of Catalyst on Diastereoselective Nitrene Insertion using 3a.[a]

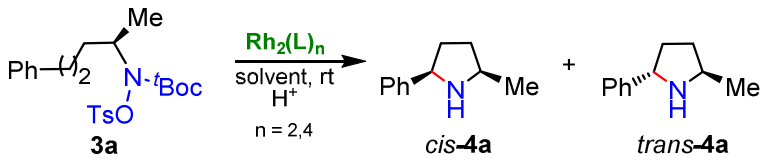

Entry	Catalyst[b]	mol%	Solvent	Yield (%)[c]	dr (cis:trans)
1	$Rh_2(esp)_2$	2.0	TFE/DCM (4:1)	73	25:75
2	$Rh_2(TFA)_4$	2.0	TFE	35	40:60
3	$Rh_2(TPA)_4$	1.0	TFE	49	36:64
4[d]	Rh_2(*S*-DOSP)$_4$	1.0	TFE/TFT (5:1)	65	10:90
5	Rh_2(*R*-BTPCP)$_4$	1.0	TFE	65	24:76
6[d]	Rh_2(*R*-PTAD)$_4$	1.0	TFE/DCM (4:1)	63	89:11
7[d]	**Rh_2(*S-tert*PTTL)$_4$**	**0.5**	**TFE/TFT (5:1)**	**60**	**>97:3**
8[d]	**$Rh_2(OAc)_4$**	**1.0**	**TFE/DCM (4:1)**	**60**	**7:93**
9[e]	$Rh_2(DBA)_4$	1.0	TFE	70	23:77

[a]Reaction conditions: Rh_2-catalyst, trifluoroacetic acid (TFA, 2 equiv), TFE plus other solvents, rt. [b]See reference 32 for ligand structures. [c]Isolated yield. [d]Camphorsulfonic acid (CSA, 15 mol%) instead of TFA. [e]*S*-enantiomer of **3a** was used instead of the *R*-enantiomer.

Table 2. Diastereoselective Synthesis of 2,5-Disubstituted Pyrrolidines via Direct C-H Nitrene Insertion.[a]

Entry	Substrate	Product	Catalyst	mol%	Solvent	Yield (%)	dr (*cis*:*trans*)
1	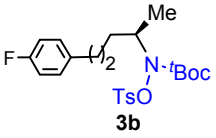 **3b**	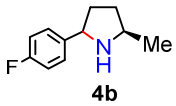 **4b**	$Rh_2(OAc)_4$	2.00	TFE/DCM (4:1)	62	5:95
			Rh_2(*S-tert*PTTL)$_4$	0.50	TFE/TFT (4:1)	62	>98:2
2	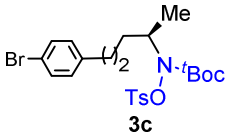 **3c**	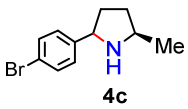 **4c**	$Rh_2(OAc)_4$	1.00	TFE/TFT (2:1)	46	8:92
			Rh_2(*S-tert*PTTL)$_4$	0.05	TFE/TFT (5:1)	52[b]	>95:5
3	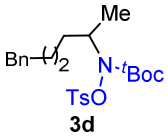 **3d**	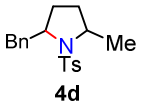 **4d**	$Rh_2(OAc)_4$	2.00	TFE/TFT (2:1)	22[c]	24:76
			$Rh_2(esp)_2$	2.00	TFE/DCM (4:1)	62[c]	30:70
			Rh_2(*S-tert*PTTL)$_4$	1.00	TFE/DCM (4:1)	62[c]	60:40
4	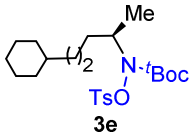 **3e**	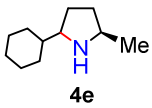 **4e**	$Rh_2(OAc)_4$	2.00	TFE/DCM (4:1)	61	15:85
			Rh_2(*S-tert*PTTL)$_4$	0.50	TFE/DCM (4:1)	70	>95:5
5	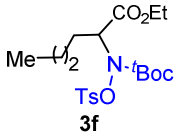 **3f**	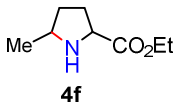 **4f**	$Rh_2(OAc)_4$	2.00	TFE/DCM (4:1)	28	23:77
			$Rh_2(esp)_2$	2.00	TFE/DCM (4:1)	59	58:42
			Rh_2(*S-tert*PTTL)$_4$	1.00	TFE/DCM (4:1)	58	63:37

[a]Reaction conditions: Rh_2-catalyst, camphorsulfonic acid (CSA, 15 mol%), rt, and TFE plus another solvent as indicated. [b]Isolated yield using 1.0 mmol of substrate at 0.25 M. [c]Derivatized for ease of isolation. Combined yield for 2 steps.

Scheme 4. Mechanistic Aspects of the Insertion.

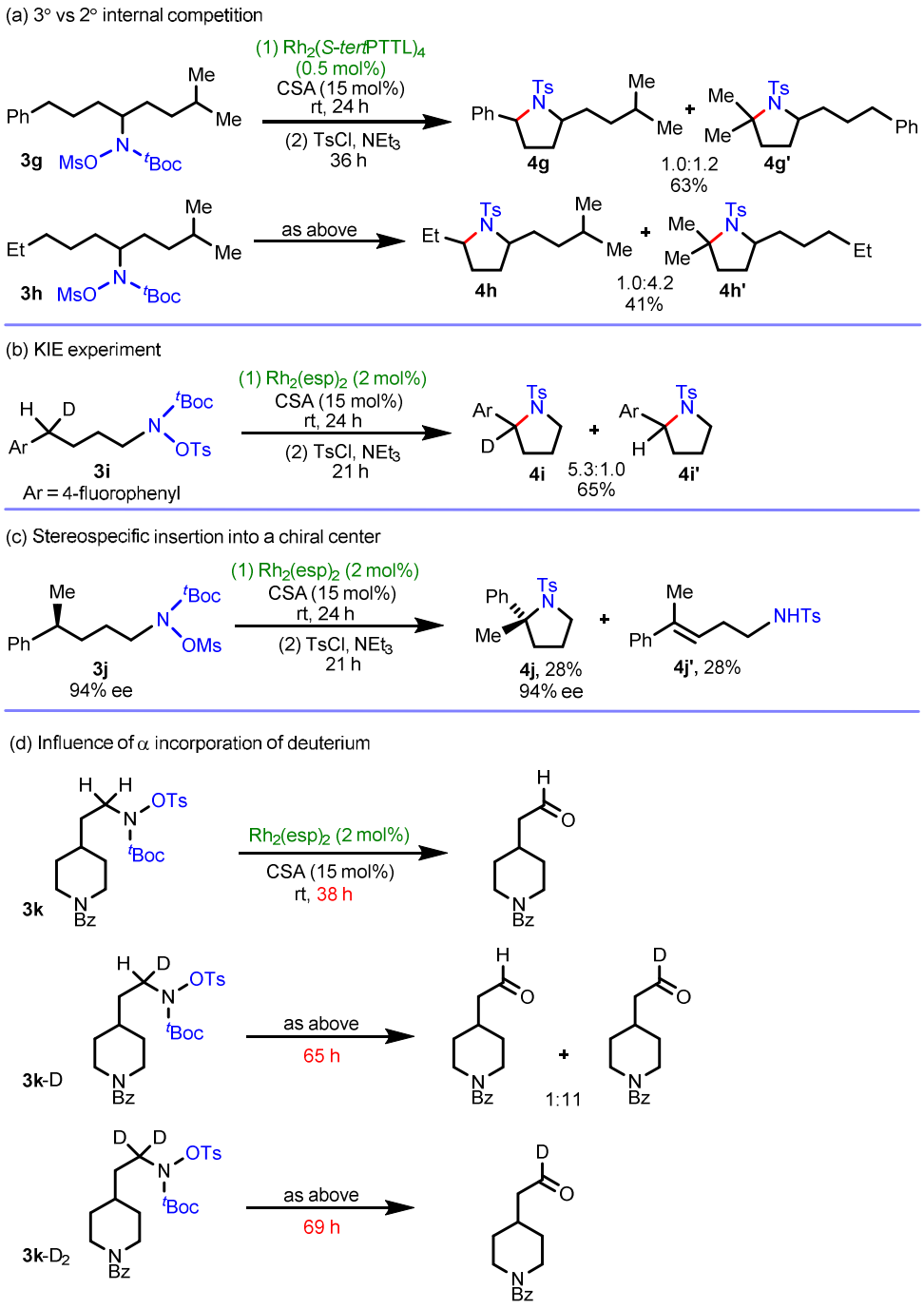

of highly *cis*-selective catalysts for future applications with a wider variety of substrates (*vide infra*).

The next phase was a comparative study using $Rh_2(OAc)_4$ and Rh_2(*S*-*tert*PTTL)$_4$ to control diastereoslectivity with a cross-section of substrates (Table 2). Both catalysts displayed excellent selectivities with *para*-substituted phenyl substrates (entries 1 and 2) even at low catalyst loadings (0.05 mol%, entry 2) on a 1.0 mmol scale. Again, insertion into an unactivated δ-methylene to form a pyrrolidine was favored over an activated ε-methylene (entry 3) or unactivated ε-methine (entry 4) to furnish piperidines. The results in entries 4 and 5 do not support a significant contribution from π-stacking interactions to stereocontrol. On the other hand, the slight, yet unexpected, preference of $Rh_2(esp)_2$ for *cis*-**4f** (entries 3 and 5) versus its *trans*-preference with **3a** (Table 1, entry 1) suggests a potential contribution of the ester group to diastereocontrol, and warrants further exploration. Generally, both $Rh_2(OAc)_4$ and Rh_2(*S*-*tert*PTTL)$_4$ maintained their respective *trans*- and *cis*-preferences, and were confirmatory for **4d** and **4f** when 1D NMR spectroscopy was ambiguous. Despite the moderate/low diastereoselectivities in entries 3 and 5, the results in Table 2 demonstrate, in select cases, a remarkable ligand-dependent discrimination between two diastereotopic acyclic sp^3 C-H bonds

and are a testament to the privileged nature of the paddlewheel structure of dirhodium catalysts (entries 1, 2, and 4). This phenomenon should find widespread applications to late stage pyrrolidine synthesis.

As shown in Scheme 3 (**2f**) and Table 2 (**4d**), the kinetic preference of the nitrenoid provides excellent regioselectivity for unactivated over activated sp^3 centers. To further explore the site-selectivity of this methodology, internal competition experiments were conducted (Scheme 4, Panel a). The availability of highly diastereoselective catalysts was beneficial in simplifying the ^{1}H NMR analyses of these experiments. Using the *cis*-selective catalyst Rh_2(*S*-*tert*PTTL)$_4$, **3g** yielded a 1.0:1.2 mixture of **4g** and **4g'** with a slight preference for the 3° versus benzylic 2° center. Notably, **4g** was isolated as a single diastereomer.[33] On the other hand, a more significant preference for 3° (4.2:1.0) was observed when internal competition was against an unactivated 2° center (**3h**). These results suggest a selectivity profile of 3°≥benzylic>2°>>1° and corresponds well with the selectivity observed with $Rh_2(OAc)_4$ catalyzed nitrene insertions of sulfamate esters.[34]

The observed site-selectivities suggest a build-up of positive charge or radical character at the reaction site since 3° and benzylic centers provide better stabilization for both radicals and carbocations. To gain further insights on this, the kinetic isotope effect (KIE) for **3i** was measured (Scheme 4, Panel b). ^{1}H NMR analysis of the crude reaction mixture and isolated **4i**/**4i'** gave a KIE of 5.3, which suggests significant C-H bond breakage in the transition state. This value is similar to that observed with Fe-dipyrrinato (KIE 5.3),[17] [Ru_2(hp)$_4$Cl] (KIE 4.9),[35] and Cu-diketiminato (KIE 5.3-6.6)[36] which are believed to occur through a stepwise mechanism, but higher than values observed with those believed to occur through a concerted mechanism (KIE 1-3).[25,37,38] Further, our observed KIE highlights a potential difference in the reactivity of unstabilized and stabilized nitrenes since nitrene transfer with sulfamate esters using $Rh_2(esp)_2$ gives a KIE of 2.9.[37,39]. In agreement with the stereospecific transformations of **1c** and **1d**, insertion into the 3° benzylic center in **3j** (Scheme 4, Panel c) occurred with no detectable loss in enantiomeric excess. However, the formation of significant quantities of olefin **4j'** suggests a competitive hydride transfer mechanism is operative. Indeed, the formation of TFE adducts (observed as side products during insertions into benzylic centers)[40] and α-insertion products to form aldehydes or ketones may be explained by a hydride transfer (HDT) mechanism. For the latter case, it was of interest[41] to determine the influence of an α-deuterium in selecting between hydrogen or hydride transfer mechanisms. Due to the significant KIE observed, it is reasonable to expect a slower α-deuterium atom transfer (DAT) or deuteride transfer (DDT) coupled with a corresponding faster δ insertion when all competing processes occur. To this end, the mono-and di-deuterated forms of **3k** were evaluated under the insertion conditions (Scheme 4, Panel d). Although a significant difference in reaction rates was observed, all three substrates gave the corresponding aldehyde as the major product, and no pyrrolidine was observed by ^{1}H NMR analyses of the crude and purified materials. We believe that the failure of this particular substrate could be due to an unfavorable conformational effect or an unidentified attribute of this insertion. Nonetheless, our data suggest a need for the rational design of catalysts able to favor HAT over HDT to further improve reaction scope and efficiency. In light of the high stereospecificity observed with **1c**, **1d**, and **3j**, as well as the high diastereoselectivity of **3a-e**, it appears that a stepwise HAT with fast radical rebound leads to productive δ-insertion while HDT results in side-product formation. With the limited amount of data, a change to a more concerted mechanism for less activated sp^3 centers cannot be completely ruled out.

As a working hypothesis, we propose the stereo- and regio-chemical outcomes of the preceding nitrenoid insertions arise from non-bonding interactions within the substrate and between the substrate and ligands of the catalyst, the combination of which determines the preferred geometry at the δ-carbon (Figure 2). Intermediate **A** (Panel a) depicts the acyclic Rh_2-nitrenoid complex with the substrate in a staggered, *anti*-conformation (an energy minimum). When the catalyst ligand R^3 is bulky (upper pathway) and in the chiral-crown conformation with all quadrants sterically hindered, steric repulsion between R^3 and R^1 favors rotamer **B** where R^1 is positioned away from the catalyst's ligands and H^b is suitably positioned for nitrene insertion leading to the *cis*-diastereomer by way of transition state **C**. As discussed above, the extent of the steric effect is dependent on the cavity size of the chiral crown catalyst; this relationship is critical for the design of highly *cis*-selective catalysts when R^1 is smaller than phenyl. For non-chiral crown catalysts, R^1 approaches the least hindered quadrant of the catalyst resulting in low or no *cis*-selectivity due to limited interaction with R^3. When R^3 is small (lower pathway) and/or a non-chiral crown catalyst, e.g, R^3 = CH_3- as in $Rh_2(OAc)_4$, is utilized, nitrene insertion into H^a via transition state **D** is favored resulting in the *trans*-diastereomer. In conformer **A** (Figure 2, Panel b), R^1 is positioned farthest from the nitrenoid and assumes an *anti*-orientation with respect to the C(3)-C(4) bond. This favors formation of five-membered rings. For larger ring sizes (>5) to be formed, R^1 would need to be positioned closest to the nitrenoid, i.e., **E**. This stereochemical model is similar to that proposed by Doyle and co-workers[42] for diastereoselective carbene C-H insertions.

CONCLUSION

The rational design of regio- and stereoselective catalysts for direct sp^3 C-H functionalization remains challenging.[43] The results presented here along with other recent developments should provide alternatives to the use of auxiliaries and directing groups and help accomplish these goals. We anticipate these results will expedite the development of predictive tools for the design of selective catalysts for other catalyst-controlled transformations involving unprotected nitrenoids (or electrophilic aminating agents).

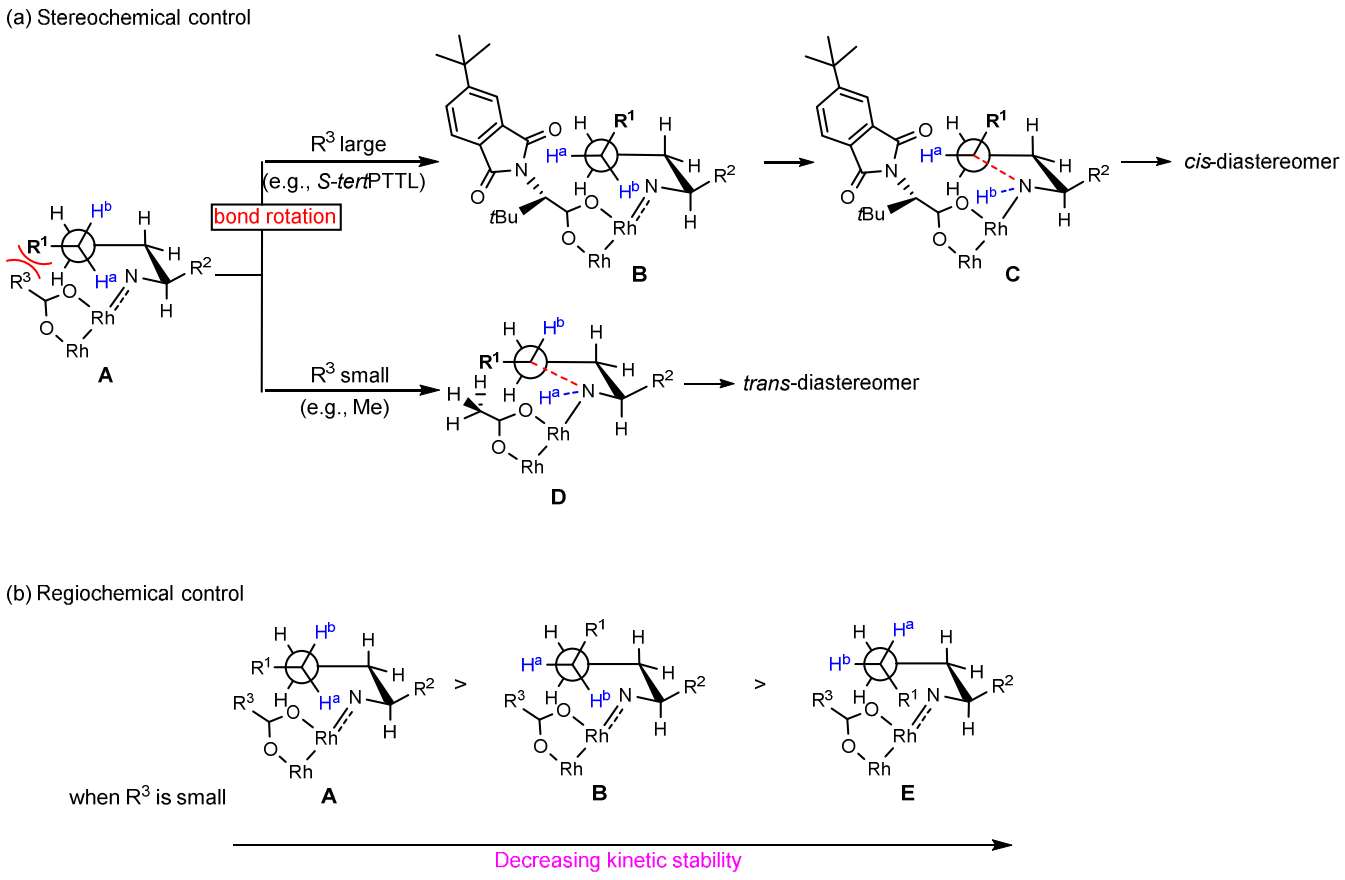

Figure 2. Working model of nitrene insertion into acyclic sp^3 C-H bonds. **(a)** Interactions between substrate and the catalyst ligands determine which diastereotopic proton undergoes nitrenoid insertion. **(b)** The prefered stereochemical conformation at C(5) determines the regioselectivity of nitrene insertion.

ASSOCIATED CONTENT

Supporting Information

The Supporting Information is available free of charge on the ACS Publications website at DOI://pubs.acs.org."
Experimental procedures and analytical data for all new compounds.
Crystallographic data for **2p** (CCDC 1571901) (CIF)

AUTHOR INFORMATION

Corresponding Author

*j.falck@utsouthwestern.edu

ORCID

Sailu Munnuri: 0000-0001-5675-6032
Adeniyi Michael Adebesin: 0000-0002-2865-2532
Mahesh P. Paudyal: 0000-0003-1025-395X
Muhammed Yousufuddin: 0000-0002-4303-8303
Alfonso Dalipe: 0000-0003-1420-447X
John R. Falck: 0000-0002-9219-7845

Author Contributions

The manuscript was written through contributions of all authors. All authors have given approval to the final version of the manuscript.

Notes

The authors declare no competing financial interest.

ACKNOWLEDGMENT

Financial support provided by the Dr. Ralph and Marian Falk Medical Research Trust Bank of America, N.A., Trustee, the Cystic Fibrosis Foundation (HURLEY16Go), NIH (RO1 HL111392), and the Robert A. Welch Foundation (Grant I-0011). Professor Michael P. Doyle is thanked for generously providing dirhodium catalysts. We thank Dr. Feng Lin for guidance with NMR spectroscopy.

REFERENCES

(1) Nakamura, I.; Yamamoto, Y. *Chem. Rev.* **2004**, *104*, 2127.
(2) Race, N. J.; Hazelden, I. R.; Faulkner, A.; Bower, J. F. *Chem. Sci.* **2017**, *8*, 5248.
(3) Musacchio, A. J.; Lainhart, B. C.; Zhang, X.; Naguib, S. G.; Sherwood, T. C.; Knowles, R. R. *Science* **2017**, *355*, 727.
(4) Michon, C.; Abadie, M-A.; Medina, F.; Agbossou-Niedercorn, F. *J. Organomet. Chem.* **2017**, *847*, 13.
(5) Hazelden, I. R.; Ma, X.; Langer, T.; Bower, J. F. *Angew. Chem. Int. Ed.* **2016**, *55*, 11198.
(6) Park, Y.; Kim, Y.; Chang, S. *Chem. Rev.* **2017**, *117*, 9247.

(7) Jat, J. L.; Paudyal, M. P.; Gao, H.; Xu, Q-L.; Yousufuddin, M.; Devarajan, D.; Ess, D. H.; Kürti, L.; Falck, J. R. *Science* **2014**, *343*, 61.

(8) Wang, H.; Yang, J. C.; Buchwald, S. L. *J. Am. Chem. Soc.* **2017**, *139*, 8428.

(9) Curto, J. M.; Kozlowski, M. C. *J. Am. Chem. Soc.* **2015**, *137*, 18.

(10) McNally, A.; Haffemayer, B.; Collins, B. S. L.; Gaunt, M. J. *Nature* **2014**, *510*, 129.

(11) Yang, M.; Su, B.; Wang, Y.; Chen, K.; Jiang, X.; Zhang, Y-F.; Zhang, X-S.; Chen, G.; Cheng, Y.; Cao, Z.; Guo, Q-Y.; Wang, L.; Shi, Z-J. *Nat. Commun.* **2014**, *5*, 4707.

(12) He, G.; Zhao, Y.; Zhang, S.; Lu, C.; Chen, G. *J. Am. Chem. Soc.* **2012**, *134*, 3.

(13) Nadres, E. T.; Daugulis, O. *J. Am. Chem. Soc.* **2012**, *134*, 7.

(14) Löffler, K.; Freytag, C. *Ber. Dtsch. Chem. Ges.* **1910**, *42*, 3427.

(15) Wolff, M. E. *Chem. Rev.* **1963**, *63*, 55.

(16) Dorta, R. L.; Francisco, C. G.; Suárez. E. *J. Chem. Soc. Chem. Commun.* **1989**, 1168.

(17) Hennessy, E. T.; Betley, T. A. *Science* **2013**, *340*, 591.

(18) Bagh, B.; Broere, D. L. J.; Sinha, V.; Kuijpers, P. F.; van Leest, N. P.; de Bruin, B.; Demeshko, S.; Siegler, M. A.; van der Vlugt, J. I. *J. Am. Chem. Soc.* **2017**, *139*, 5117.

(19) Broere, D. L. J.; de Bruin, B.; Reek, J. N. H.; Lutz, M.; Dechert, S.; van der Vlugt, J. I. *J. Am. Chem. Soc.* **2014**, *136*, 11574.

(20) Paudyal, M. P.; Adebesin, A. M.; Burt, S. R.; Ess, D. H.; Ma, Z.; Kürti, L.; Falck, J. R. *Science* **2016**, *353*, 1144.

(21) Zoidis, G.; Tsotinis, A.; Kolocouris, N.; Kelly, J. M.; Prathalingam, S. R.; Naesens, L.; De Clercq, E. *Org. Biomol. Chem.* **2008**, *6*, 3177.

(22) Wawzonek, S.; Thelen, P. J. *J. Am. Chem. Soc.* **1950**, *72*, 2118.

(23) Elofson, R. M.; Gadallah, F. F.; Laidler, J. K. *Can. J. Chem.* **1987**, *65*, 2770.

(24) Jeffrey, J. L.; Sarpong, R. *Chem. Sci.* **2013**, *4*, 4092.

(25) Roizen, J. L.; Harvey, M. E.; Du Bois, J. *Acc. Chem. Res.* **2012**, *45*, 911.

(26) Collet, F.; Lescot, C.; Liang, C.; Dauban, P. *Dalton Trans.* **2010**, *39*, 10401.

(27) Lebel, H.; Spitz, C.; Leogane, O.; Trudel, C.; Parmentier, M. *Org. Lett.* **2011**, *13*, 5460.

(28) Qin, C. M.; Davies, H. M. L. *J. Am. Chem. Soc.* **2014**, *136*, 9792.

(29) DeAngelis, A.; Dmitrenko, O.; Yap, G. P. A.; Fox, J. M. *J. Am. Chem. Soc.* **2009**, *131*, 7230.

(30) Lindsay, V. N. G.; Lin, W.; Charette, A. B. *J. Am. Chem. Soc.* **2009**, *131*, 16383.

(31) Adly, F. G.; Gardiner, M. G.; Ghanem, A. *Chem. Eur. J.* **2016**, *22*, 3447.

(32) Ligand structures:

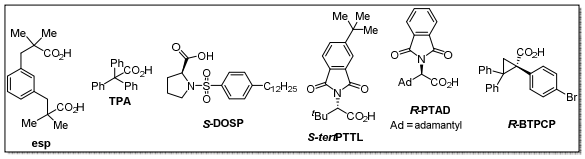

(33) The corresponding reaction with $Rh_2(OAc)_4$ gave *cis*-and *trans*-**4g** in a 1:6 ratio. See supporting information for details.

(34) Fiori, K. W.; Espino, C. G.; Brodsky, B. H.; Du Bois, J. Tetrahedron **2009**, *65*, 3042.

(35) Harvey, M. E.; Musaev, D. G.; Du Bois, J. *J. Am. Chem. Soc.* **2011**, *133*, 17207.

(36) Badiei, Y. M.; Dinescu, A.; Dai, X.; Palomino, R. M.; Heinemann, F. W.; Cundari, T. R.; Warren, T. H. *Angew. Chem. Int. Ed.* **2008**, *47*, 9961.

(37) Varela-Álvarez, A.; Yang, T.; Jennings, H.; Kornecki, K. P.; MacMillan, S. N.; Lancaster, K. M.; Mack, J. B. C.; Du Bois, J.; Berry, J. F.; Musaev, D. G. *J. Am. Chem. Soc.* **2016**, *138*, 2327.

(38) Rigoli, J. W.; Weatherly, C. D.; Alderson, J. M.; Vo, B. T.; Schomaker, J. M. *J. Am. Chem. Soc.* **2013**, *135*, 17238.

(39) It should be noted that the generation of a distinct active catalyst under the reaction conditions could be an alternative explanation for the observed differences in KIE.

(40) See supporting information for details.

(41) The authors thank the reviewers for suggesting this experiment.

(42) Doyle, M. P.; Kalinin, A. V.; Ene, D. G. *J. Am. Chem. Soc.* **1996**, *118*, 8837.

(43) Attempted intermolecular C-H amination using the reagents and conditions described herein have failed to date.

Table of Contents artwork

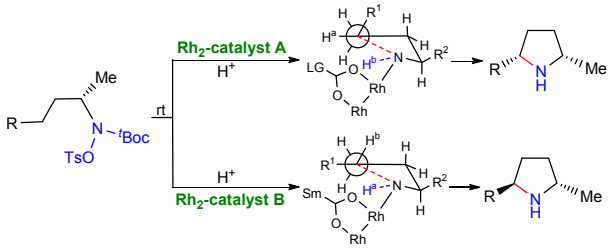

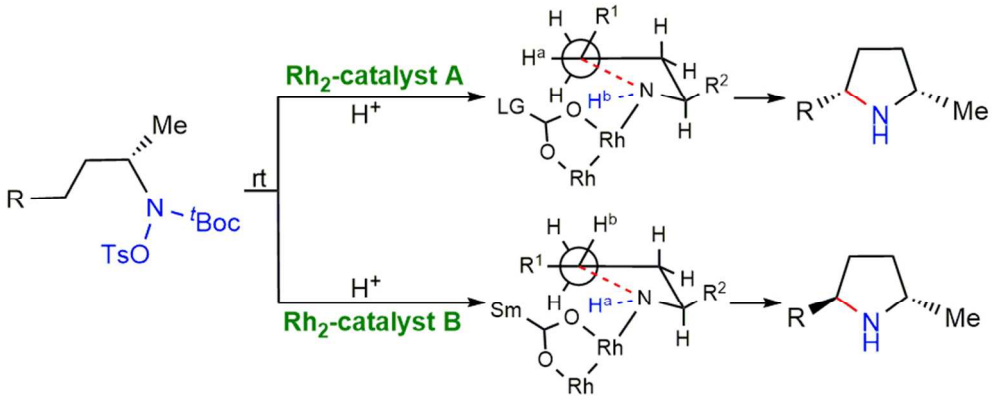

80x33mm (300 x 300 DPI)